

HDR imaging pipeline for spectral filter array cameras

Jean-Baptiste Thomas^{1,2}, Pierre-Jean Lapray³, and Pierre Gouton¹

¹ Université de Bourgogne, Franche-Comté,
LE2I, Dijon, France

² The Norwegian Colour and Visual Computing Laboratory,
NTNU - Norwegian University of Science and Technology, Gjøvik, Norway

³ MIPS Laboratory, Université de Haute Alsace,
Mulhouse, France

Abstract. Multispectral single shot imaging systems can benefit computer vision applications in needs of a compact and affordable imaging system. Spectral filter arrays technology meets the requirement, but can lead to artifacts due to inhomogeneous intensity levels between spectral channels due to filter manufacturing constraints, illumination and object properties. One solution to solve this problem is to use high dynamic range imaging techniques on these sensors. We define a spectral imaging pipeline that incorporates high dynamic range, demosaicing and color image visualization. Qualitative evaluation is based on real images captured with a prototype of spectral filter array sensor in the visible and near infrared.

Keywords: Multispectral imaging, spectral filter arrays, high dynamic range, imaging pipeline

1 Introduction

Spectral filter arrays (SFA) technology [22] provides a compact and affordable mean to acquire multispectral images (MSI). Such images have been proven to be useful in countless applications, but their extended use to general computer vision application was limited due to complexity of imaging set-up, calibration and specific imaging pipelines and processing. In addition, spectral videos are not easily handled either. SFA, however, is developed around a very similar imaging pipeline than color filter arrays (CFA), e.g. RGB, which is rather well understood and already implemented in many solutions. Indeed, SFA, similarly to CFA, is a spatio-spectral sampling of the scene captured in a single shot of a solid-state, single, image sensor. In this sense, SFA may provide a conceptual solution that improves vision systems.

Up to recently, only simulations of SFA camera were available, which made its experimental evaluation and validation difficult. Recent works on optical filters [29, 45, 8] in parallel to the development of SFA camera prototypes in the visible electromagnetic range [15], in the near infrared (NIR) [9] and in combined visible and NIR [20, 43] permitted the commercialization of solutions, e.g.

Imec [12], Silios [41], Pixelteq [31]. In addition, several color cameras include custom filter arrays that are in-between CFA and SFA (e.g. [13, 28]). We could then consider that the use of SFA technology may reach a large scale of use soon after the development of standard imaging pipelines and drivers.

We address and demonstrate the imaging pipeline in this communication. One remaining limitation of SFA is to preserve the energy balance between channels [30, 21] while capturing a scene. Indeed, due to the large number of filters and their spectral characteristics, *i.e.* narrow band sensitivities and inadequacy with the scene and illumination, or large inhomogeneity between filter shapes, it is frequent to observe one or several channels under- or over-exposed for a given integration time, which is common to all filters. This may be solved in theory by optimizing the filters before creating the sensor [21]. But filter realization is not yet flexible enough. Another way to solve this issue would be to develop sensors with by-pixel integration control. This is in development within some 3D silicon sensor concepts [16, 5], but this technology is at its very beginning, despite of recent developments.

On the other hand, in gray-level and color imaging, the problem of under and over-exposure of parts of the scene is addressed by means of high dynamic range (HDR) imaging [24, 6]. HDR imaging permits to potentially recover the radiance of the scene independently of the range of intensities present in the scene. As the dynamic range of a given sensor is limited, the quantization of the radiance values is a source of problems. The signal detection of very low intensity is limited by the dark noise. On the other hand, high intensities of the input signal can not be completely recovered and are sometimes voluntarily ignored (saturated pixels). To overcome these problems, a low exposure time image could be used to discretize the highest intensities, whereas a longer exposure time allows quantifying well relatively low light signals.

In an ideal configuration, an HDR image is simply obtained by bringing Low Dynamic Range (LDR) images in the same domain by dividing each image by its particular exposure time (normalization), and then by summing the corresponding pixel values. However, due to the effect of electronic circuits, most of the cameras have a non-linear processing regarding to the digitization of intensities into integer values. This non-linear transformation is materialized by the camera response function, denoted by $g(i)$, where i indexes the pixel value. It is assumed that this curve is monotonic and smooth. Some algorithms have been developed to recover this characteristic [6, 27, 35]. The most common method is the non-parametric technique from Debevec *et al.* [6]. For a given exposure time and intensity value, the relative radiance value is estimated by using $g(i)$ and a weighting function $\omega(i)$. Debevec *et al.* use a "hat" function as weighting function (see Figure 6(b)), based on the assumption that mid-range pixels (values close to 128 for an 8-bit sensor) are the most reliable and the best exposed pixel for a given scene and integration time. In addition, recent advances have been done on the capture and processing of HDR video with low latency, using hardware-based platforms [25, 18, 19]. For HDR video, merging images captured at different times could lead to ghost artefacts when there are moving objects. This has been

largely studied in recent years [1, 3]. So, we argue that such methodology could be embedded in the SFA imaging pipeline without breaking the advantages of SFA technology for computer vision.

HDR multispectral acquisition is already treated by e.g. Brauers *et al.* [4] and Simon [39]. However, they consider the problem of HDR using individual bands acquired sequentially, so each band is treated independently. In the case of SFA, we may consider specific joined processes. Our contribution is to define the imaging pipeline to SFA and to provide results on real experimental data.

In this communication, we first generalize the imaging CFA pipeline to SFA. This new SFA imaging pipeline incorporates HDR concept based on multiple exposure images, in Section 2. Then, the experimental implementation is shown in Section 3, which is based on real images, acquired by a SFA system spanning the visible and NIR range [43]. Results are discussed in Section 4, before we conclude in Section 5.

2 Imaging Pipelines

In this section, we describe different imaging pipelines from CF to HDR-SFA.

2.1 CFA Imaging Pipeline

Several CFA imaging pipelines exist. We can classify them in two large groups: one concerns the hardware and real-time processing community [44, 46, 33], the other concerns the imaging community [38, 32, 14]. A very general distinction is that the former one often demosaics the raw image in very early steps, conversely the latter demosaics after or jointly with other processings such as white balance. In this work we base our design after the generic imaging pipeline defined by Ramanath *et al.* [32], which is shown in Figure 1.

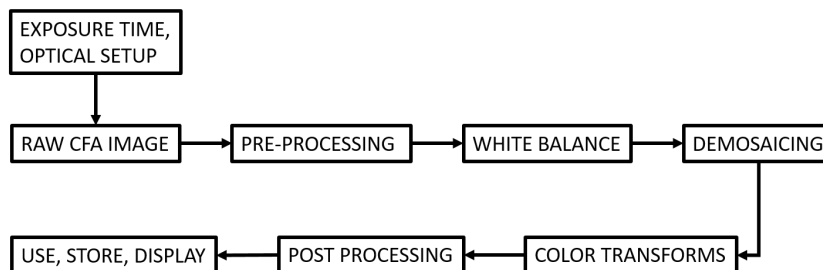


Fig. 1. CFA imaging pipeline similarly defined as in [32]. The pipeline contains pre-processing on raw data, which include for instance a dark noise correction and other denoising. Raw data would be corrected for illumination before to be demosaiced. Images are then projected into an adequate color space representation and followed by some post-processing, e.g. image enhancement, before to get out of the pipeline.

2.2 HDR-CFA Imaging Pipeline

HDR imaging has been developed mostly within monochromatic sensors for acquisition. However, there is a huge amount of work that developed the tone mapping of HDR color images for visualization, (e.g. [34, 40]), the HDR capture is mostly an intensity process performed per channel [39]. We propose to encapsulate a general HDR-CFA imaging pipeline such as shown in Figure 2. This pipeline is based on sequence of images of the same scene having different integration times. We argue that a HDR pipeline may have two distinguished output: one leads to HDR radiance images, which can be stored and used for automatic applications. The other leads to a display-friendly visualization of color image. Note that the two outputs may overlap in specific applications.

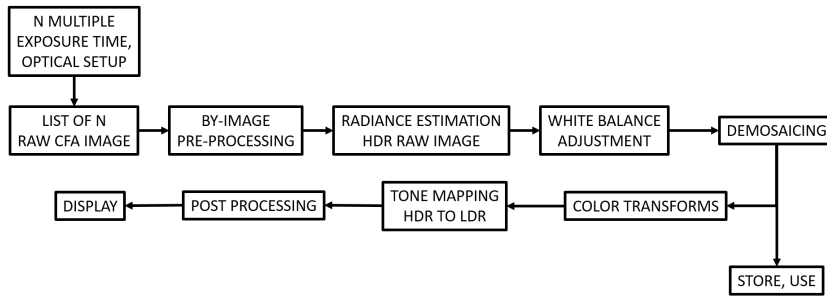


Fig. 2. HDR-CFA imaging pipeline. In this case, the denoising is typically performed per image similarly to the LDR-CFA case. Then, radiance estimation is performed based on the multiple images, providing radiance raw images. White balancing and demosaicing is performed on this data. Then, the HDR image may be used as is, or continue into a visualization pipeline, where a color transform, tone-mapping and image-enhancement may be applied before visualization.

2.3 SFA Imaging Pipeline

SFA sensors are currently investigated and developed, however beside demosaicing and applications dedicated processing, the rest of the pipeline is not very well defined, nor understood. We argue that a similar pipeline to CFA may be considered, which is defined in Figure 3.

2.4 HDR-SFA Imaging Pipeline

According to the introductory discussion, we propose to extend the SFA pipeline to an HDR version in order to benefit from HDR, in particular towards a better balance between channel sensitivities. We propose to consider the raw image and to treat it as a gray-level image for relative radiance estimation. Thus, we perform all radiance reconstruction prior to any separation between bands. The pipeline is defined in Figure 4.

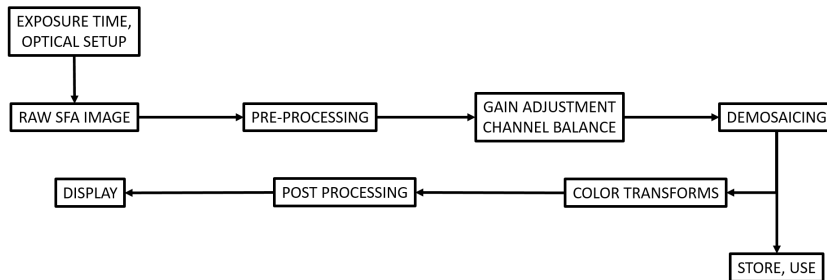


Fig. 3. SFA imaging pipeline. At the instar of CFA, this pipeline defines some illumination discarding process and demosaicing. The spectral image would be typically used for application after demosaicing. However, these data may not be observable as they are, so the pipeline is prolonged for visualization. The color transform is ought to be slightly different than CFAs, for several more channel and NIR information may be present in the spectral image.

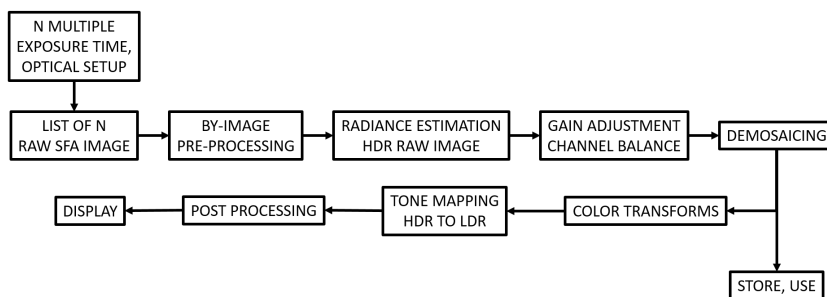


Fig. 4. HDR-SFA imaging pipeline. The radiance estimation is performed on the raw image taken as a whole and not per channel. This leads to a raw HDR image, which may be corrected for illumination and demosaiced. Then, the HDR multispectral image may be stored or used. The visualization process projects the data into a HDR color representation of the data, which is tone-mapped and processed for visualization.

3 Implementation of the HDR-SFA Imaging Pipeline

This section explicitly defines which processing is embedded in each of the pipeline boxes. We take well-established and understood methods from the state of the art in order to provide benchmarking proposal and analysis. These methods are combined into the pipeline. Our proposal is not exclusive in the sense that any method may be used and different orders may also be considered.

The prototype SFA camera from Thomas *et al.* [43] is used in this study. Sensitivities are shown in Figure 5(a). Spatial arrangement and other details may be found in their article. The raw images are pre-processed and denoised according to what is performed in this article, which is basically a dark noise removal. Then, following the pipeline, HDR data are computed. Subsection 3.1 covers the HDR data recovering. HDR images are demosaiced, according to Miao *et al.* [26]

algorithm, forming the full resolution HDR multispectral image. The part of the pipeline that concerns visualization is developed in Subsection 3.2.

3.1 HDR generation

Debevec radiance reconstruction [6] is probably the most understood HDR imaging pipeline. The model is based on the assumption that pixel values can be related to the quantity of radiance, by using a computed camera response function, which is recovered through a self calibration method. So before reconstructing HDR images, the camera response function must be estimated. To recover this response curve, we capture 8 LDR bracketed images⁴ at different exposure times, from 0.125 ms to 16 ms with a one-stop increment, see Figure 5(b).

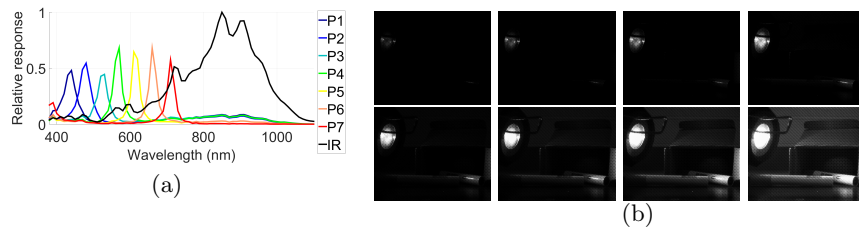


Fig. 5. (a) The spectral camera response from Thomas *et al.* [43]. (b) The complete set of LDR raw mosaiced images acquired with these exposure times: $\{0.125, 0.25, 0.5, 1, 2, 4, 8, 16\}$ ms (all spaced by one stop). These exposures are used to calculate the global response curves of our camera, shown in Figure 6(a).

The algorithm from Debevec is based on the solution of a set of linear equations by the singular value decomposition method. The usual algorithm is generally applied on RGB cameras, and it recovers 3 different response curves, one by channel. In our case, as we have 8 spectral channels, we recover 8 curves (see Figure 6(a)). We notice that the dispersion is relatively low among channels, so in the following, we use the median value of these curves for all channels, allowing us to work directly on the raw data at once to generate HDR values.

As described in the pipeline in Figure 4, we recover relative radiance values directly from preprocessed data (called "raw data"). A number of 3 exposure times are selected. We chose only 3 exposures because it is a number commonly used in the literature [3, 25], as it gives relatively high dynamic range and not too much ghost effects. The radiance values are recovered using the response curve, and by combining the pixel value with the corresponding exposure time (c.f. Debevec equation [6]). A weighted sum of radiance values among all exposure

⁴ We could work with three images as later in this work, but it is commonly accepted that using more images than necessary can lead to a better response curve estimation in terms of robustness to noise.

times is done using the hat weighting function (see Figure 6(b)), to give more contribution to mid range pixel intensities during the HDR reconstruction. The single raw-HDR image is then demosaiced to recover the whole spatial resolution for each HDR band. We have obtained a HDR multispectral image.

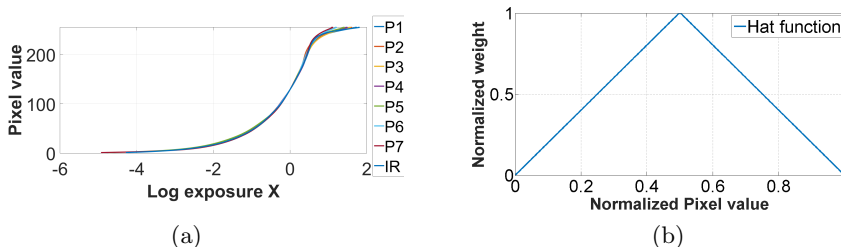


Fig. 6. (a) Response functions recovered from the image set shown in Figure 5(b) for each of the bands $P_{1-7,IR}$. (b) The well-exposedness hat function used in our experiment.

3.2 Visualization procedure

HDR spectral data are projected into an HDR coded CIEXYZ color space according to a color transform based on the 24 Gretag Macbeth color checker patches reflectance and the scene acquisition illumination measured in situ. This colorimetric image may be either transformed into sRGB directly or tone mapped by a more efficient algorithm. In the following, we use two tone mapping as examples, one is a global logarithmic mapping from Duan *et al.* [7], the other is from Krawczyk *et al.* [17], and combines global and local tone mapping processing⁵.

3.3 Other pipeline components

One obvious gain adjustment would be defined by the sensitivity curves efficiency ratio. Some works are also initiated toward spectral constancy [42]. These works are under development, and for benchmarking purpose, we decided to keep the ratio untouched in this study.

Post-processing, except the tone-mapping, are avoided in this article, but may consider spectral demultiplexing [37, 36], image enhancement such as ghost removal [10] or other items.

Spectral LDR data are stored into multiband Tiff files. Spectral HDR data are stored using 32-bit Tiff files (8 channels). To provide a direct visualization with a great number of software implementing tone-mapping solutions, RGB HDR data are also computed, encoded within ".hdr" RGBE [23] format.

We assume color data to be displayed onto a 8 bit display. The pipeline may be adapted to the new generation of HDR displays that rose up on the market.

⁵ We used the code which is implemented in the Matlab HDR Toolbox [2].

4 Results

We provide examples of resulting images for two scenes in Figure 7 and Figure 8. Due to space constraint, the description is embedded into the captions of the figures.

5 Conclusion

We generalized the imaging pipeline to SFA cameras. We demonstrated that a very similar to CFA architecture can be used for SFA successfully, which is encouraging for the industrial development of solutions based on this technology, for either spectral reconstruction and traditional computer vision tasks.

Further works include to evaluate the impact of each of the imaging pipeline components with respect to either visualization or usability of the HDR data. We only presented one instantiation, while many are possible. Further works include also standardization of camera and pipeline as well as file format and transmission line. Other aspect lies in the development of quality of HDR spectral data. Although there exists some work for HDR images [11], little work consider HDR spectral data.

References

1. An, J., Ha, S.J., Cho, N.I.: Probabilistic motion pixel detection for the reduction of ghost artifacts in high dynamic range images from multiple exposures. *EURASIP Journal on Image and Video Processing* 2014(1), 42 (2014)
2. Banterle, F., Artusi, A., Debattista, K., Chalmers, A.: *Advanced High Dynamic Range Imaging: Theory and Practice*. AK Peters (CRC Press), Natick, MA, USA (2011)
3. Bouderbane, M., Lapray, P.J., Dubois, J., Heyrman, B., Ginhac, D.: Real-time ghost free HDR video stream generation using weight adaptation based method. In: *Proceedings of the 10th International Conference on Distributed Smart Camera*. pp. 116–120. *ICDSC '16*, ACM, New York, NY, USA (2016)
4. Brauers, J., Schulte, N., Bell, A., Aach, T.: Color accuracy and noise analysis in multispectral HDR imaging. In: *14. Workshop Farbbildverarbeitung 2008*. pp. 33–42. Shaker Verlag (2008)
5. Brochard, N., Nebhen, J., Ginhac, D.: 3D-IC: New perspectives for a digital pixel sensor. In: *Proceedings of the 10th International Conference on Distributed Smart Camera*. pp. 92–97. *ICDSC '16*, ACM, New York, NY, USA (2016)
6. Debevec, P.E., Malik, J.: Recovering high dynamic range radiance maps from photographs. In: *Proceedings of the 24th Annual Conference on Computer Graphics and Interactive Techniques*. pp. 369–378. *SIGGRAPH '97*, ACM Press/Addison-Wesley Publishing Co., New York, NY, USA (1997)
7. Duan, J., Bressan, M., Dance, C., Qiu, G.: Tone-mapping high dynamic range images by novel histogram adjustment. *Pattern Recognition* 43, 1847–1862 (2010)
8. Eichenholz, J.M., Dougherty, J.: Ultracompact fully integrated megapixel multi-spectral imager. In: *SPIE OPTO: Integrated Optoelectronic Devices*. pp. 721814–721814. International Society for Optics and Photonics (2009)

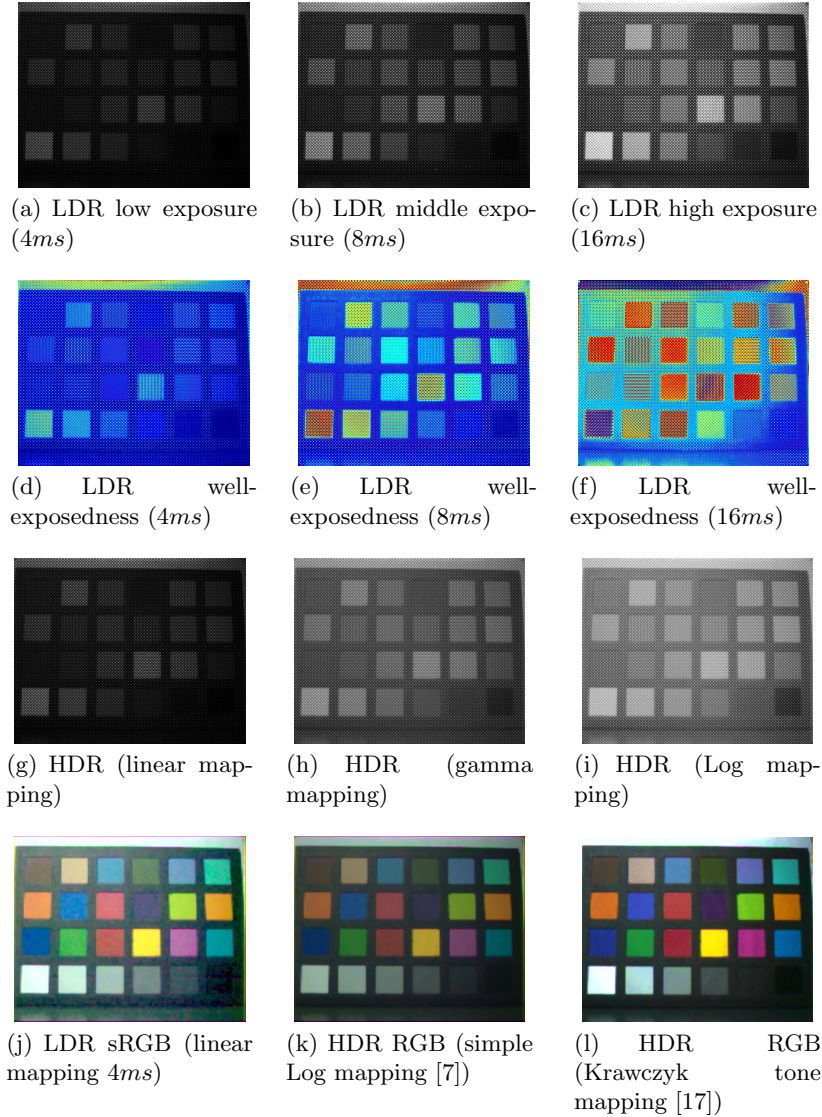


Fig. 7. Results for the MacBeth color chart (typically a low dynamic range scene). (a,b,c) Raw images, (d,e,f) false color well-exposedness representation, (g,h,i) HDR generation results from the 3 exposure set (a,b,c), (j,k,l) sRGB representation of both LDR and HDR data for comparison. The important issue, that we try to solve in this work, is that if we look the raw images at a neutral MacBeth patch, we can clearly distinguish the inherent energy balance problems between pixel values through the 8 channels. This phenomenon is highlighted in Figure 7(d),7(e) and 7(f), where a pixel position could hold a good intensity for a given exposure time (red color), and a bad exposition in another (blue color). It leads to visual noise when visualizing a single LDR reconstructed image (Figure 7(j)). Our HDR-SFA imaging pipeline can correct this problem by a certain amount, which is visually appreciated.

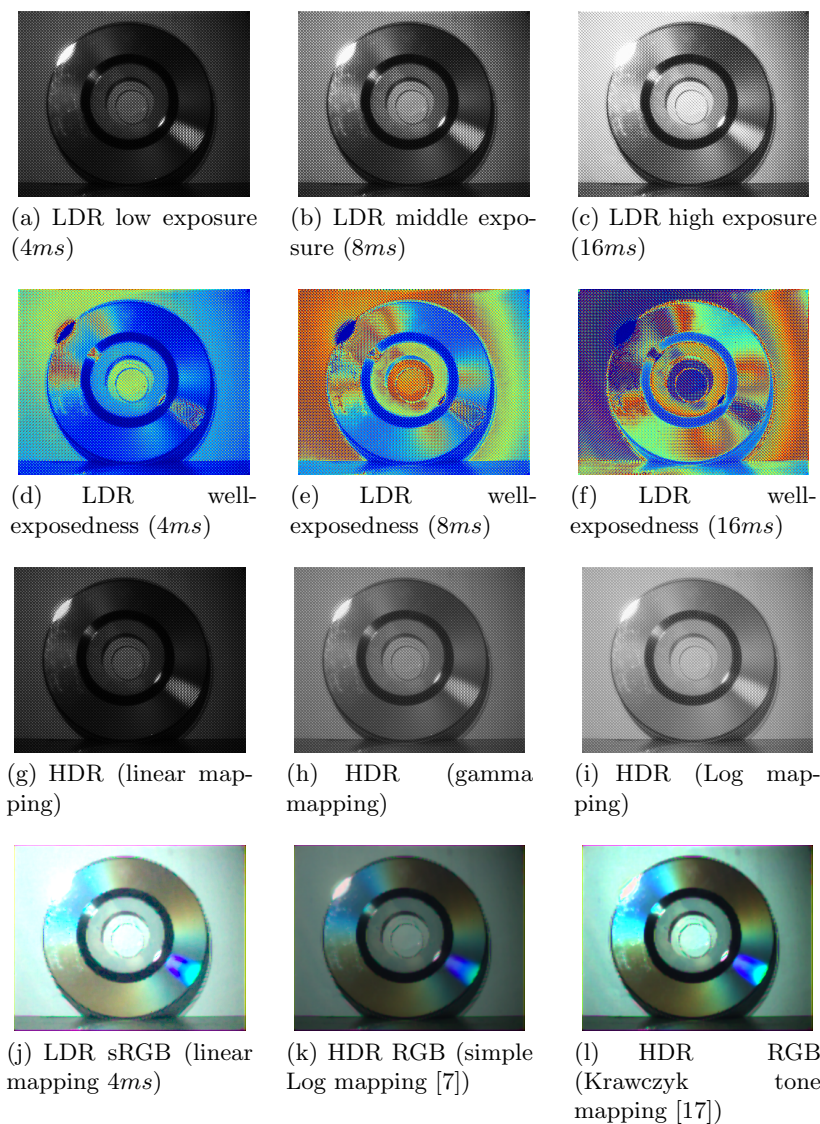


Fig. 8. Results for the CD scene (relatively high dynamic range scene compared to the previous MacBeth scene). (a,b,c) Raw images, (d,e,f) false color well-exposedness representation, (g,h,i) HDR generation results from the 3 exposure set (a,b,c), (j,k,l) sRGB representation of both LDR and HDR data for comparison. As for Figure 7, we show that channels are inequitably affected by signal noise among exposures. Showing different good or bad pixel intensities, there is the necessity to take several exposure times in order to equalize the distribution of noise between channels. Contrary to the MacBeth scene, which is a typical low dynamic range scene, we can see in addition that some areas with high specular reflection have less saturated pixels in the resulting HDR image. We still observe saturated pixels at specular directions, which saturates the lowest integration time.

9. Geelen, B., Blanch, C., Gonzalez, P., Tack, N., Lambrechts, A.: A tiny VIS-NIR snapshot multispectral camera. In: SPIE OPTO. pp. 937414–937414. International Society for Optics and Photonics (2015)
10. Granados, M., Kim, K.I., Tompkin, J., Theobalt, C.: Automatic noise modeling for ghost-free HDR reconstruction. *ACM Transactions on Graphics (TOG)* 32(6), 201 (2013)
11. Hanhart, P., Bernardo, M.V., Pereira, M., G. Pinheiro, A.M., Ebrahimi, T.: Benchmarking of objective quality metrics for HDR image quality assessment. *EURASIP Journal on Image and Video Processing* 2015(1), 39 (2015)
12. IMEC: hyperspectral-imaging, <http://www2.imec.be>
13. Jia, J., Barnard, K.J., Hirakawa, K.: Fourier spectral filter array for optimal multispectral imaging. *IEEE Transactions on Image Processing* 25(4), 1530–1543 (April 2016)
14. Kao, W.C., Wang, S.H., Chen, L.Y., Lin, S.Y.: Design considerations of color image processing pipeline for digital cameras. *IEEE Transactions on Consumer Electronics* 52(4), 1144–1152 (Nov 2006)
15. Kiku, D., Monno, Y., Tanaka, M., Okutomi, M.: Simultaneous capturing of RGB and additional band images using hybrid color filter array. In: Proc. SPIE. vol. 9023, pp. 90230V–90230V–9 (2014)
16. Knickerbocker, J.U., Andry, P., Dang, B., Horton, R., Patel, C.S., Polastre, R., Sakuma, K., Sprogis, E., Tsang, C., Webb, B., et al.: 3D silicon integration. In: 2008 58th Electronic Components and Technology Conference. pp. 538–543. IEEE (2008)
17. Krawczyk, G., Myszkowski, K., Seidel, H.P.: Lightness perception in tone reproduction for high dynamic range images. In: *Computer Graphics Forum*. vol. 24, pp. 635–645. Wiley Online Library (2005)
18. Lapray, P.J., Heyrman, B., Ginhac, D.: HDR-ARTiSt: an adaptive real-time smart camera for high dynamic range imaging. *Journal of Real-Time Image Processing* pp. 1–16 (2014)
19. Lapray, P.J., Heyrman, B., Ginhac, D.: Hardware-based smart camera for recovering high dynamic range video from multiple exposures. *Optical Engineering* 53(10), 102110 (2014)
20. Lapray, P.J., Thomas, J.B., Gouton, P.: A multispectral acquisition system using MSFAs. *Color and Imaging Conference 2014(2014)*, 97–102 (2014-11-03T00:00:00)
21. Lapray, P.J., Thomas, J.B., Gouton, P., Ruichek, Y.: Energy balance in spectral filter array camera design. *Journal of the European Optical Society* (2017)
22. Lapray, P.J., Wang, X., Thomas, J.B., Gouton, P.: Multispectral filter arrays: Recent advances and practical implementation. *Sensors* 14(11), 21626 (2014)
23. Larson, G.W., Shakespeare, R.: *Rendering with Radiance: the art and science of lighting visualization*. Booksurge Llc (2004)
24. Mann, S., Picard, R.: Being undigital with digital cameras: Extending dynamic range by combining differently exposed pictures. In: *Proceedings of IS&T 46th annual conference*. pp. 422–428 (1995)
25. Mann, S., Lo, R.C.H., Ovtcharov, K., Gu, S., Dai, D., Ngan, C., Ai, T.: Realtime HDR (high dynamic range) video for eyetap wearable computers, FPGA-based seeing aids, and glasseyes (eyetaps). In: *Electrical & Computer Engineering (CCECE), 2012 25th IEEE Canadian Conference on*. pp. 1–6. IEEE (2012)
26. Miao, L., Qi, H., Ramanath, R., Snyder, W.E.: Binary tree-based generic demosaicking algorithm for multispectral filter arrays. *IEEE Transactions on Image Processing* 15(11), 3550–3558 (Nov 2006)

27. Mitsunaga, T., Nayar, S.K.: Radiometric self calibration. In: CVPR, 1999. IEEE Computer Society Conference on. vol. 1, p. 380 Vol. 1 (1999)
28. Monno, Y., Kikuchi, S., Tanaka, M., Okutomi, M.: A practical one-shot multi-spectral imaging system using a single image sensor. *IEEE Transactions on Image Processing* 24(10), 3048–3059 (Oct 2015)
29. Park, H., Dan, Y., Seo, K., Yu, Y.J., Duane, P.K., Wober, M., Crozier, K.B.: Vertical silicon nanowire photodetectors: Spectral sensitivity via nanowire radius. In: CLEO: Science and Innovations. pp. CTh3L–5. OSA (2013)
30. Péguillet, H., Thomas, J.B., Gouton, P., Ruichek, Y.: Energy balance in single exposure multispectral sensors. In: CVCS 2013. pp. 1–6 (Sept 2013)
31. PIXELTEQ: Micro-patterned optical filters, <https://pixelteq.com/>
32. Ramanath, R., Snyder, W.E., Yoo, Y., Drew, M.S.: Color image processing pipeline. *IEEE Signal Processing Magazine* 22(1), 34–43 (Jan 2005)
33. Rani, K.S., Hans, W.J.: FPGA implementation of bilinear interpolation algorithm for CFA demosaicing. In: Communications and Signal Processing (ICCSP), 2013 International Conference on. pp. 857–863. IEEE (2013)
34. Reinhard, E., Stark, M., Shirley, P., Ferwerda, J.: Photographic tone reproduction for digital images. *ACM Transactions on Graphics* 21(3), 267–276 (2002)
35. Robertson, M.A., Borman, S., Stevenson, R.L.: Dynamic range improvement through multiple exposures. In: Image Processing, 1999. ICIP 99. Proceedings. 1999 International Conference on. vol. 3, pp. 159–163. IEEE (1999)
36. Sadeghipoor, Z., Lu, Y.M., Mendez, E., Ssstrunk, S.: Multiscale guided deblurring: Chromatic aberration correction in color and near-infrared imaging. In: Signal Processing Conference (EUSIPCO), 2015 23rd European. pp. 2336–2340 (Aug 2015)
37. Sadeghipoor, Z., Thomas, J.B., Ssstrunk, S.: Demultiplexing visible and near-infrared information in single-sensor multispectral imaging. *Color and Imaging Conference 2016*, xx–xx (2016-11-03T00:00:00)
38. Sharma, G., Trussell, H.J.: Digital color imaging. *IEEE Transactions on Image Processing* 6(7), 901–932 (1997)
39. Simon, P.M.: Single Shot High Dynamic Range and Multispectral Imaging Based on Properties of Color Filter Arrays. Ph.D. thesis, University of Dayton (2011)
40. Tamburrino, D., Alleysson, D., Meylan, L., Ssstrunk, S.: Digital camera workflow for high dynamic range images using a model of retinal processing. In: Electronic Imaging 2008. pp. 68170J–68170J. International Society for Optics and Photonics (2008)
41. TECHNOLOGIES, S.: Micro-optics supplier, <http://www.silios.com/>
42. Thomas, J.B.: Illuminant estimation from uncalibrated multispectral images. In: CVCS 2015. pp. 1–6. IEEE (2015)
43. Thomas, J.B., Lapray, P.J., Gouton, P., Clerc, C.: Spectral characterization of a prototype SFA camera for joint visible and NIR acquisition. *Sensors* 16(7), 993 (2016)
44. Tsin, Y., Ramesh, V., Kanade, T.: Statistical calibration of CCD imaging process. In: Computer Vision, 2001. ICCV 2001. Proceedings. Eighth IEEE International Conference on. vol. 1, pp. 480–487. IEEE (2001)
45. Yi, D., Kong, L., Wang, J., Zhao, F.: Fabrication of multispectral imaging technology driven MEMS-based micro-arrayed multichannel optical filter mosaic. In: SPIE MOEMS-MEMS. pp. 792711–792711. International Society for Optics and Photonics (2011)
46. Zhou, J.: Getting the most out of your image-processing pipeline. White Paper, Texas Instruments (2007)